Available online at www.sciencedirect.com
SCIENCE DIRECT®
International Journal of Heat and Mass Transfer 47 (2004) 2699–2714
International Journal of HEAT and MASS TRANSFER
www.elsevier.com/locate/ijhmt

Double-diffusive natural convection in parallelogrammic enclosures filled with fluid-saturated porous media

V.A.F. Costa *

Departamento de Engenharia Mecânica, Universitário de Aveiro, Campus Universitdáio de Santiago, 3810-193 Aveiro, Portugal

Received 27 January 2003; received in revised form 28 November 2003

Abstract

Enclosures of parallelogrammic shape present high potential to be used in heat and/or mass transfer applications, as they can act as heat and/or mass transfer inhibitors or promoters, being usually referred to as heat and/or mass transfer diodes. The heat and/or mass transfer characteristics and performances of such enclosures depend mainly on the imposed boundary conditions and geometrical arrangement. In this work, the double-diffusive natural convection problem in parallelogrammic enclosures filled with fluid-saturated porous media is studied numerically. The pressure–velocity link for the fluid contained within the fluid-saturated porous media is modeled using the Darcy Law, and a discussion is presented about the use of this model. Emphasis is given to the situation when the porous media that fill the enclosure are saturated with moist air. A short set of values of the dimensionless governing parameters for steady two-dimensional parallelogrammic enclosures is taken, and analysis is concentrated over the numerical results obtained for such combinations of governing parameters. The situations of combined or opposite global heat and mass flows are considered. Results clearly show the strong potential of parallelogrammic enclosures filled with fluid-saturated porous media for heat and mass transfer applications. Such single parallelogrammic enclosures can be assembled, thus giving rise to complete, and even complex, efficient heat and/or mass transfer systems.

1. Introduction

Numerical studies on double-diffusive natural convection in enclosures filled with fluid-saturated porous media are present in many recent works [1–10], just to mention a few. However, to the author's knowledge, no studies have been conducted considering enclosures of parallelogrammic shape. Depending on the inclination angle, aspect ratio and imposed boundary conditions at the vertical walls of the enclosure, different (or even very different) heat and/or mass transfer characteristics and performances can be achieved. Under given imposed boundary conditions, very different heat and/or mass transfer performances are obtained for positive or for negative inclination angles, maintaining fixed the remaining parameters and conditions. Due to this marked directional behavior, the parallelogrammic enclosure is usually referred to as a heat and/or mass transfer diode.

Single thermal natural convection problem in parallelogrammic enclosures has been previously studied [11–16]. Some of such studies include additional effects of heat diffusive separation walls between contiguous parallelogrammic enclosures assembled in a vertical stack [11,14]. Double-diffusive natural convection in parallelogrammic enclosures has been studied recently by the same author [17], where it is presented a short summary of the previous work made on natural convection in enclosures of this shape. Work reported in [17] clearly shows the marked directional behavior of the parallelogrammic enclosures in what concerns both heat and/or mass transfer. It is thus a geometrical form that needs to be explored and that can be used as the basic form from which, by assembly, complete and/or complex efficient heat and/or mass transfer systems can be obtained. The present work is the counter-part of the work reported in [17], now dealing with parallelogrammic enclosures

* Tel.: +351-234-370-829; fax: +351-234-370-953.
E-mail address: v_costa@mec.ua.pt (V.A.F. Costa).

0017-9310/$ - see front matter © 2004 Elsevier Ltd. All rights reserved.
doi:10.1016/j.ijheatmasstransfer.2003.11.031

Nomenclature

C	concentration
D	mass diffusivity
g	gravitational acceleration
Da	Darcy number
H	height
H	heatfunction
k	thermal conductivity
K	permeability
L	length
Le	Lewis number
m	mass
M	molar mass
M	massfunction
n	outward normal
N	buoyancy ratio
Nu	Nusselt number
p	pressure
Pr	Prandtl number
Ra	Darcy-modified Rayleigh number
Sc	Schmidt number
Sh	Sherwood number
T	temperature
u, v	Cartesian velocity components
W	specific humidity, dry basis
x, y	Cartesian co-ordinates

Greek symbols

α	thermal diffusivity
β	volumetric expansion coefficient
θ	inclination angle
ν	kinematic viscosity
ρ	density
ψ	streamfunction

Subscripts

C	referring concentration
H	higher value
L	lower value
T	referring temperature
*	dimensionless

filled with fluid-saturated porous media, some common aspects being present in both works.

Enclosures filled with fluid-saturated porous media are common in many fields. In many cases, the porous media are saturated with moist air, which is almost always present. Construction elements and insulation systems are two of the most frequent situations of this type. Starting with enclosures of parallelogrammic shape, filled with air-saturated porous media (insulation materials), one can obtain panels by assembling many of such enclosures. Due to the heat and/or mass transfer directional behavior of each individual enclosure, the so obtained panels also have a directional behavior, the panels behaving as heat and/or mass transfer diodes. Such composite panels can be used with advantage, once established the way as they should act when compared with panels obtained as assembling of enclosures of rectangular shape: heat and/or mass transfer promoters or inhibitors. The use of the parallelogrammic shape in construction elements is just one possibility among many others. This is the main reason to study the double-diffusive natural convection problem in enclosures of parallelogrammic shape, filled with a fluid-saturated porous media. The presented results correspond to some selected combinations of the dimensionless governing parameters, for which, in addition, the temperature and concentration boundary conditions can be specified such that global heat and mass flows that cross the enclosure are combined or opposite. The temperature and concentration buoyancy effects can also be combined or opposite, the presented results being limited to combined buoyancy effects only. Analysis is made for the results obtained for some particular cases, but the presented model is general.

Visualization of the heat and mass transfer processes is made in detail using the heatlines and masslines [18]. The global Nusselt and Sherwood numbers dependence on the dimensionless governing parameters and boundary conditions is explored in detail. Combinations of the dimensionless governing parameters and boundary conditions leading to multiple solutions or oscillatory solutions [7–10] are deliberately avoided.

2. Physical and numerical modeling

2.1. Physical model

The two-dimensional parallelogrammic enclosure filled with a fluid-saturated porous medium, as presented in Fig. 1, which is under the influence of the vertical gravity field, is the domain under analysis. The fluid saturating the porous medium is a perfect mixture of an indifferent fluid and a solute whose mass transfer occurs. Vertical walls, of height H, are maintained at constant different levels of temperature and concentration, thus leading to a double-diffusive natural convection problem. Inclined walls of length L form an angle θ relative to the horizontal, being referred to as *inclined walls*, and are assumed to be impermeable and adiabatic. Inclina-

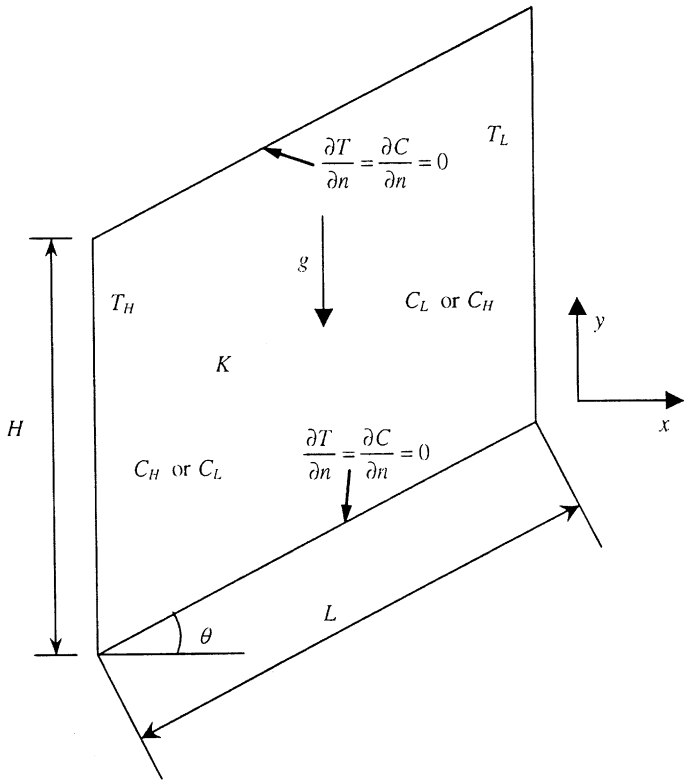

Fig. 1. Physical model and geometry.

tion angle θ and aspect ratio H/L are changed in order to analyze their influence on the resulting flow structure and on heat and mass transfer performances of the parallelogrammic enclosures.

2.2. Model assumptions

The fluid saturating the porous medium is a perfect two-component mixture, and this mixture is taken as a Newton–Fourier fluid. The solute concentration is taken as the ratio between the mass of solute to the total mass, $C = m_1/(m_1 + m_2)$. If the mixture under analysis is the moist air, C is the specific humidity in a wet basis, which is related to the specific humidity in a dry basis, W, as $C = W/(1 + W)$. The mixture density is not affected by pressure changes (incompressible mixture), but it changes under temperature and/or concentration changes. Eventual phase changes inside the enclosure are not considered. The porous medium is assumed to be isotropic, and characterized by a uniform permeability, K. The pressure–velocity link for the fluid contained within the saturated porous medium is given by the Darcy Law, a model whose discussion is made in Section 2.5.

Density on the buoyancy term is a function of temperature and concentration, being taken into account through the Boussinesq approach. The volumetric thermal expansion coefficient is obtained as $\beta_T = -(\partial\rho/\partial T)_{p,C}/\rho$ and similarly, the volumetric mass expansion coefficient relative to concentration C is obtained as $\beta_C = -(\partial\rho/\partial C)_{p,T}/\rho$. The mixture density in the buoyancy term is then expressed as [19]

$$\rho = \rho_L[1 - \beta_T(T - T_L) - \beta_C(C - C_L)] \quad (1)$$

Usually $\beta_T \geqslant 0$, the water in the range 0–4.1 °C being the most frequent exception, β_C can be either positive or negative. For a perfect mixture of ideal gases, $\beta_T = 1/T_{abs}$ and $\beta_C = (M_2 - M_1)/[(M_2 - M_1)C + M_1]$, M_1 being the molecular weight of the transported solute and M_2 the molecular weight of the indifferent fluid. For moist air at room conditions, β_T can assume values near $\beta_T = 0.0034$ °C^{-1} and β_C can assume values between $\beta_C = 0.61$ kg/kg (for pure dry air, with $C = 0$) and $\beta_C = 0.38$ kg/kg (for pure water vapor, with $C = 1$).

The thermophysical properties of the involved media are assumed to be constant, exception made to density appearing in the buoyancy term, as explained before. In practical situations, however, the properties of the mixture in each point are dependent, between others, of the concentration level of the transported species and of the temperature level.

It is assumed that the thermal levels are small and similar enough so that thermal radiation heat transfer between the walls is negligible, and the fluid is assumed to be radiatively non-participating. The energy terms due to viscous dissipation and change of temperature due to reversible deformation (work of pressure forces) are not considered. For the two-component mixture under analysis, there are not considered the energy terms of interdiffusional convection and diffusion thermo (Dufour effect) [20]. The only considered energy diffusion term is thus this due to Fourier conduction. The only considered mass transfer diffusional term is this due to Fick diffusion, and the pressure diffusion, body force diffusion and thermal diffusion (Soret effect) terms are not considered [20].

The presented results for moist air must be used with care in practical situations, due to the real possibility of the non-considered condensation of the transported species (water vapor). Temperature and concentration levels can be obtained that lead to relative humidities close to the unit (or even greater than 1), situations for which condensation of the transported species occur. Such eventual phase change, however, is not taken into account in the present work.

2.3. Model equations

Assuming that the pressure–velocity link for the fluid within the porous medium is given by the Darcy Law, it can be stated that

$$u = -\frac{K}{\mu}\left(\frac{\partial p}{\partial x}\right); \quad v = -\frac{K}{\mu}\left(\frac{\partial p}{\partial y} + \rho g\right) \tag{2}$$

where K is the permeability of the isotropic porous medium. Defining the streamfunction through its first order derivatives as

$$\rho u = \frac{\partial \psi}{\partial y}; \quad \rho v = -\frac{\partial \psi}{\partial x} \tag{3}$$

taking into account the Boussinesq approach and making the involved variables dimensionless as

$$u_* = u/(\alpha/H) = \partial \psi_*/\partial y_*; \quad v_* = v/(\alpha/H) = -\partial \psi_*/\partial x_* \tag{4}$$

$$x_* = x/H; \quad y_* = y/H \tag{5}$$

$$\begin{aligned} T_* &= (T - T_L)/(T_H - T_L); \\ C_* &= (C - C_L)/(C_H - C_L) \end{aligned} \tag{6}$$

$$\psi_* = \psi/\rho\alpha \tag{7}$$

the set of partial differential equations governing the problem under analysis is

$$0 = \frac{\partial^2 \psi_*}{\partial x_*^2} + \frac{\partial^2 \psi_*}{\partial y_*^2} + Ra_T \frac{\partial}{\partial x_*}(T_* + NC_*) \tag{8}$$

$$\frac{\partial}{\partial x_*}(u_* T_*) + \frac{\partial}{\partial y^*}(v_* T_*) = \frac{\partial^2 T_*}{\partial x_*^2} + \frac{\partial^2 T_*}{\partial y_*^2} \tag{9}$$

$$\frac{\partial}{\partial x_*}(u_* C_*) + \frac{\partial}{\partial y_*}(v_* C_*) = \frac{1}{Le}\left(\frac{\partial^2 C_*}{\partial x_*^2} + \frac{\partial^2 C_*}{\partial y_*^2}\right) \tag{10}$$

In these equations α is the thermal diffusivity of the combined fluid plus solid porous matrix medium, in this work taken as nearly equal to the thermal diffusivity of the fluid alone.

The following dimensionless parameters emerge from the governing equations

$$Le = \alpha/D \tag{11}$$

$$Ra_T = \frac{g\beta_T(T_H - T_L)KH}{\nu\alpha} \tag{12}$$

$$N = \frac{\beta_C(C_H - C_L)}{\beta_T(T_H - T_L)} \tag{13}$$

where Ra_T is the Darcy-modified Rayleigh number. This parameter can be expressed as $Ra_T = \lfloor g\beta_T(T_H - T_L)H^3/(\nu\alpha)\rfloor(K/H^2)$, the number within the square brackets being the Rayleigh number usual in natural convection heat transfer in non-porous domains, and the ratio $Da = K/H^2$ being usually referred to as the Darcy number.

Parameter N is the buoyancy ratio, which is the ratio between the solute and thermal buoyancy forces. It can be either positive or negative, its sign depending of that of the ratio between the volumetric temperature and concentration expansion coefficients, β_T and β_C, respectively. When N is positive, the temperature and concentration buoyancy effects are combined, and they are opposite otherwise. When Eqs. (9) and (10) have the same boundary conditions, the T_* and C_* fields are coincident if $Le = 1$.

Combined global heat and mass flows and negative values of parameter N can lead to multiple solutions or oscillatory solutions [7–10]. For N close to the unit with opposite global heat and mass flows, one can have also multiple solutions. Considering, for example, the linear initial distributions $T_* = 1 - x_*$ and $C_* = x_*$, one obtains $T_* + NC_* = 1$, a result that is independent of x_*. All the points in the enclosure are under the same buoyancy effect, and a stagnant fluid situation results. Any small disturbances, introduced by the initial conditions or by the numerical method of resolution used, lead to different flow structures because they are generating differences in an initially expected uniform buoyancy field. Such situations are intentionally avoided in the present work.

2.4. Boundary conditions

Over all the (impermeable) walls of the enclosure it is

$$\psi_* = 0 \tag{14}$$

It is thus assumed that the solute mass flow through the vertical walls is small enough in order to validate the use of zero normal velocity values at such walls. Bejan [21] presents a scale-based analysis of such an assumption. The dimensionless velocity components are made null at the walls of the enclosure, and in the interior of the domain they are evaluated from the dimensionless streamfunction using Eq. (4).

Prescription of T_* and C_* over the vertical walls can lead to a situation of combined or opposite global heat and mass flows. Over the vertical walls it is thus prescribed that

$$T_*(0,y_*)=1;\quad T_*[\cos\theta/(H/L),y_*]=0 \tag{15}$$

$$C_*(0,y_*)=1;\quad C_*[\cos\theta/(H/L),y_*]=0 \quad \text{for combined global heat and mass flows} \tag{16}$$

or

$$C_*(0,y_*)=0;\quad C_*[\cos\theta/(H/L),y_*]=1 \quad \text{for opposite global heat and mass flows.} \tag{17}$$

At the inclined walls of the enclosure, taken as adiabatic and impermeable, it is

$$\frac{\partial T_*}{\partial n_*}=\frac{\partial C_*}{\partial n_*}=0 \tag{18}$$

where n_* is the dimensionless normal to the inclined wall under consideration.

2.5. Discussion on the physical model used

The use of the Darcy Law to express the pressure–velocity link for the fluid saturating the porous medium is a reasonable model if the fluid velocity is maintained within low limits. If this is not the case, inertial effects growth and need to be taken into account using, for example, the Forchheimer modification [22]. Some recent works consider the non-Darcian effects when dealing with natural convection flows in fluid-saturated porous media [1,2,5], which generally use a Brinkman–Forchheimer equation [22].

The use of the Darcy Law seems to be a good approach if $Re_K=vK^{1/2}/\nu<1$ [22,23]. As given in [22], the vertical velocity scale corresponding to height H, near a single vertical wall, can be expressed as $v\sim(\alpha/H)Ra_T\langle 1,N\rangle=[g\beta(T_H-T_L)K/\nu]\langle 1,N\rangle$, where $\langle 1,N\rangle=\max(1,N)$. The Reynolds number based on this velocity scale is $Re_K=vK^{1/2}/\nu\sim Ra_T\langle 1,N\rangle\sqrt{Da}/Pr$, and the use of the Darcy Law seems to be a good approach if $Ra_T\langle 1,N\rangle\times\sqrt{Da}/Pr<1$, in an order of magnitude sense. For the situations under analysis, the worst situation to apply the Darcy flow model is that corresponding to the highest value of $N=5$ (that leads to the highest velocity). In this case, for a fluid with $Pr\approx 1$, the criterion to apply the Darcy flow model becomes $5Ra_T\sqrt{Da}<1$, that is $5[g\beta_T/(v\alpha)]\Delta TK^{3/2}<1$. For air at room conditions, that is, $g\beta_T/(v\alpha)\approx 10^8\ \mathrm{m^{-3}\,{}^\circ C^{-1}}$ [19], and the application criterion becomes $5\Delta TK^{3/2}<10^{-8}\ \mathrm{m^3\,{}^\circ C}$. The worst temperature difference is its maximum value, taken as the maximum temperature difference for which the Boussinesq approach can be applied, which is $\Delta T_{max}\approx 10\ {}^\circ C$, and the applicability criterion of the Darcy flow model becomes $5K<10^{-6}\ \mathrm{m^2}$, in an order of magnitude sense. Looking on the permeability of some usual porous insulation materials [22,23], one concludes that the Darcy flow model can be used in the situations under analysis.

The use of the Darcy Law poses a problem at the solid impermeable domain boundaries, where the velocity components are zero, but the pressure gradient components are not. So, the Darcy Law is not really used in the closest neighboring of the impermeable and non-slip boundaries. The velocity components are made explicitly zero at such boundaries, and they are not evaluated from the derivatives of the streamfunction field. The impermeable boundary condition $\psi_*=0$ is, however, imposed at all the walls of the enclosure.

2.6. Heat and mass transfer parameters

The global Nusselt and Sherwood numbers for the parallelogrammic enclosure are defined respectively as

$$Nu=\frac{\int_0^H -k\left(\frac{\partial T}{\partial x}\right)_{x=0}\mathrm{d}y}{k[(T_H-T_L)/L]H\cos\theta}=-\frac{1}{(H/L)\cos\theta}\int_0^1\left(\frac{\partial T_*}{\partial x_*}\right)_{x_*=0}\mathrm{d}y_* \tag{19}$$

$$Sh=\frac{\int_0^H \rho D\left|\frac{\partial C}{\partial x}\right|_{x=0}\mathrm{d}y}{\rho D[(C_H-C_L)/L]H\cos\theta}=\frac{1}{(H/L)\cos\theta}\int_0^1\left|\frac{\partial C_*}{\partial x_*}\right|_{x_*=0}\mathrm{d}y_* \tag{20}$$

As the inclined walls are impermeable and adiabatic, the derivatives $\partial T_*/\partial x_*$ and $\partial C_*/\partial x_*$ present in the global Nusselt and Sherwood numbers definitions can be equally taken at $x_*=0$ or at $x_*=\cos\theta/(H/L)$. The modulus sign was introduced when defining the Sherwood number in order to define a positive value for this parameter, for both the situations of combined or opposite global heat and mass flows. The reference situation for heat transfer, present in the denominator of Eq. (19), is the pure conduction situation through the stagnant fluid of thermal conductivity k, under the thermal gradient $(T_H-T_L)/L$, considering that the best value for the cross-section heat conduction area is $1\times H\cos\theta$, which is the adequate value for shallow

parallelogrammic enclosures. The reference situation for mass transfer, used in the definition of the Sherwood number, is obtained in a similar way.

2.7. Numerical modeling

The numerical method used in this work is an adaptation of a two-dimensional laminar version of the control-volume-based finite element method described in [24]. Iteration by iteration, the dimensionless streamfunction field is evaluated by solving Eq. (8), the dimensionless velocity components are evaluated from the dimensionless streamfunction using Eq. (4), and the dimensionless temperature and concentration fields are evaluated by solving their corresponding differential equations [Eqs. (9) and (10)]. A non-uniform structured 101×101 mesh, which expands from the walls towards the center of the enclosure in both directions with an expansion factor of 1.05, was selected after some preliminary testes of asymptotic type.

The used control volume finite element method has been tested and successfully used to solve similar problems, using primitive variables or the streamfunction together with the Darcy flow model [24–27].

3. Results and analysis

3.1. Considered situations

There are five dimensionless parameters governing the problem under analysis: Le, N, Ra_T, H/L, and θ. Additionally, both situations of combined or opposite global heat and mass flows can be considered, as given by Eqs. (16) and (17). All the presented results refer to moist air saturating the porous medium, with a low concentration of water vapor, thus fixing $Le = 0.8$. For moist air, $(M_2 - M_1) > 0$, $\beta_C \geqslant 0$, and $N \geqslant 0$. In this work are thus considered situations with combined temperature and concentration buoyancy effects only.

The expression for Ra_T can be written as $Ra_T = [g\beta_T/(v\alpha)]\Delta THK$. As $g\beta_T/(v\alpha) \approx 10^8$ m^{-3} °C^{-1} for air at room conditions [19], it is $Ra_T = 10^8\ \Delta THK$ where, as shown before when discussing the Darcy flow model, $\Delta T < 10$ °C and $5K < 10^{-6}$ m^2. For the situation with $K = 10^{-7}$ m^2, $\Delta T = 10$ °C and $H = 1$ m (a large-size enclosure), it is $Ra_T = 100$, which is taken as the upper limit for this parameter. Lower permeability, temperature difference or enclosure size lead to lower values of Ra_T, the lower value of this parameter considered in this work being $Ra_T = 25$. However, lower values of this parameter can be obtained in practical applications. The buoyancy ratio is given by Eq. (13), and the considered values for this parameter are obtained from that expression. As $\beta_T \approx 3.4\times10^{-3}$ °C^{-1} and $\beta_C = 0.61$ kg/kg for air with low moisture content, it is $N \approx 179.4(\Delta T/\Delta C)$. Many values can be obtained for the buoyancy ratio, in this work being taken $N = 5$ as the upper limit and $N = 0$ (no solute transfer) as the lower limit. In what concerns the H/L ratio, it goes from the *square* enclosure with $H/L = 1$ to the shallow enclosure with $H/L = 0.1$. It should also be noted that the limits of Ra_T and H/L taken in the present work are the same as taken by Bejan [19] to the enclosure of rectangular cross-section.

Analysis of results is concentrated on the influence of parameters N, Ra_T, H/L and θ over the resulting flow structure and on the heat and mass transfer performances of the parallelogrammic enclosures. The situation of opposite global heat and mass flows is also shortly considered.

Analysis of results presents many common features as for the double-diffusive natural convection in parallelogrammic enclosures filled with a single fluid, as described in [17].

3.2. Flow structure, temperature and concentration fields, and heat and mass transfer visualization

The flow structure is analyzed through the dimensionless streamlines, the temperature and concentration fields are analyzed through their respective dimensionless contour plots, and the heat and mass transfer processes are analyzed through the dimensionless heatlines and masslines, respectively. The marked influence of the governing dimensionless parameters and boundary conditions over the involved fields and processes is illustrated for a short set of results. Heatfunction is made dimensionless as $H_* = H/[k(T_H - T_L)]$ and massfunction is made dimensionless as $M_* = M/[\rho D(C_H - C_L)Le]$, where k is the thermal conductivity of the combined fluid plus solid porous matrix medium, in this work taken as nearly equal to the thermal conductivity of the fluid alone. As the reference diffusion situations used to make these functions dimensionless are different from the ones used to define the Nusselt and Sherwood numbers through Eqs. (19) and (20), the numeric values of such functions do not match the numerical values of the global Nusselt and Sherwood numbers [18,19].

For the *square* $H/L = 1$ parallelogrammic enclosure with $\theta = 30°$, $Ra_T = 100$ and no solute transfer ($N = 0$), the streamlines, isotherms and heatlines are presented in Fig. 2. Such results present some common features as for the differentially heated square enclosure [25], and it is evident the influence of the inclination angle over the variable's fields. It is observed some symmetry on the streamlines and on the isotherms, which also exists for the differentially heated square enclosure [28].

Results for $Ra_T = 100$, $N = 0$, $H/L = 0.25$ and $\theta = 30°$ or $\theta = -30°$ are presented in Fig. 3a (for $\theta = 30°$) and Fig. 3b (for $\theta = -30°$). For $\theta = 30°$, changing from $H/L = 1$ to $H/L = 0.25$ results in marked changes on the flow structure, the streamlines extending now

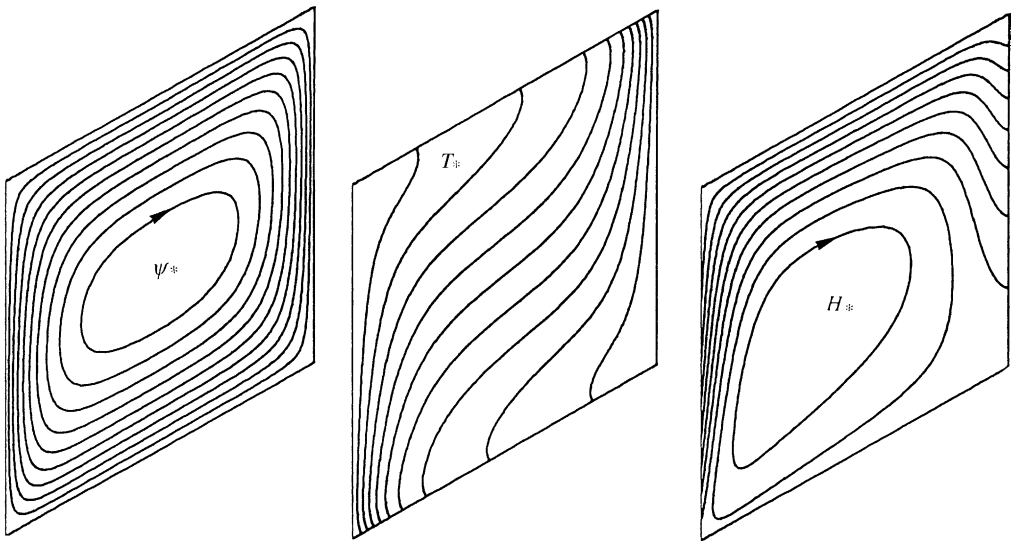

Fig. 2. Streamlines (left), isotherms (center) and heatlines (right), for the situation of non-solute transfer ($N = 0$), and $\theta = 30°$, $H/L = 1$ and $Ra_T = 100$ ($\psi_{*,min} = -5.52$, $\psi_{*,max} = 0.00$, $\Delta\psi_* = 0.55$, $\Delta T_* = 0.10$; $H_{*,min} = -1.13$, $H_{*,max} = 3.48$, $\Delta H_* = 0.46$).

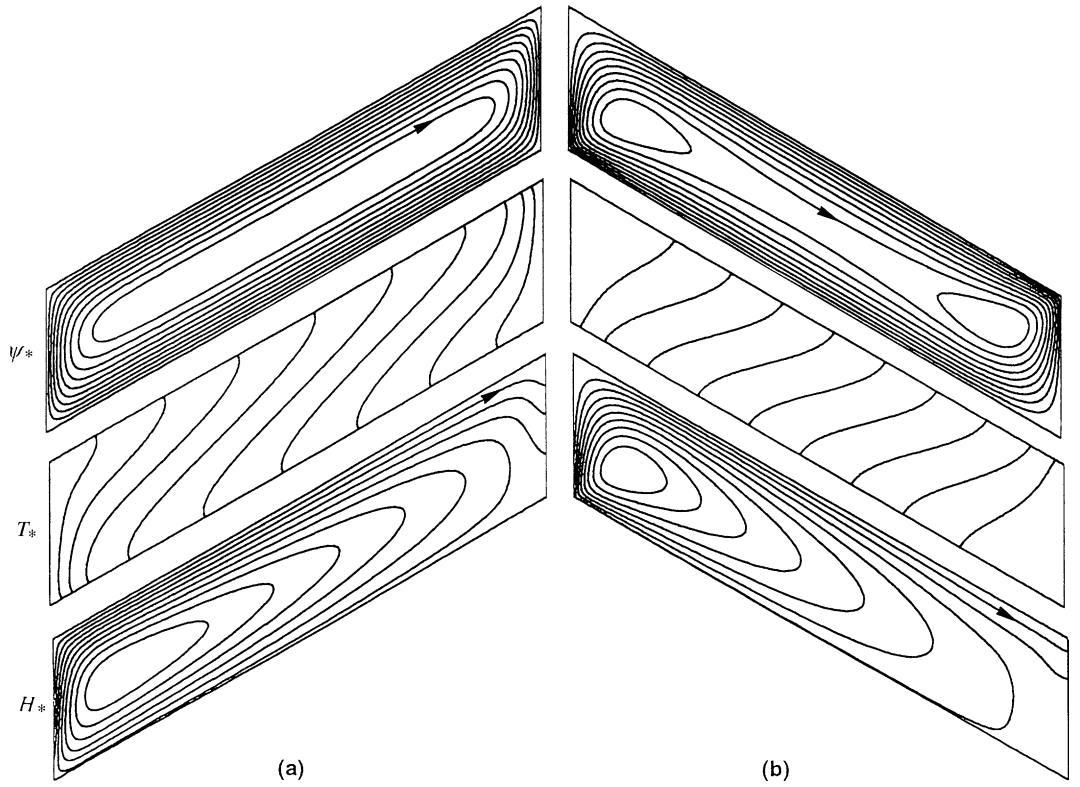

Fig. 3. Streamlines (top), isotherms (center) and heatlines (bottom), for the situation of non-solute transfer ($N = 0$), $H/L = 0.25$, $Ra_T = 100$ and (a) $\theta = 30°$ ($\psi_{*,min} = -3.54$, $\psi_{*,max} = 0.00$, $\Delta\psi_* = 0.35$, $\Delta T_* = 0.10$; $H_{*,min} = -1.96$, $H_{*,max} = 1.09$, $\Delta H_* = 0.31$); and (b) $\theta = -30°$ ($\psi_{*,min} = -1.19$, $\psi_{*,max} = 0.00$, $\Delta\psi_* = 0.12$; $\Delta T_* = 0.10$, $H_{*min} = -0.84$, $H_{*,max} = 0.35$, $\Delta H_* = 0.12$).

over almost all length L. At the center of the enclosure, the closed loops of the streamlines are close to the rectangular form, and not to the elliptical form as for the parallelogrammic enclosure with $H/L = 1$. In what

concerns the temperature field, its basic structure is essentially maintained, the isotherms being almost *parallel* to each other along the enclosure's length. Changes on the streamlines are also observed over the heatlines, which are now much more elongated, and heat flows mainly along the neighboring of the top inclined wall of the enclosure towards the right (cold) wall. When inclination angle changes from $\theta = 30°$ to $\theta = -30°$, maintaining $H/L = 0.25$, marked changes occur in all the process. Flow structure changes, presenting now a main clockwise vortex with two minor interior vortexes near the hot and cold vertical walls. Flow is less intense than for $\theta = 30°$, as given by the numeric values of the streamfunction. Temperature field presents a marked stratification, the isotherms being nearly horizontal and *parallel* to each other. Heat flows mainly by conduction across the enclosure, thus resulting in a low global heat flow. This same conclusion can also be obtained from the numeric values of the heatlines. Heatlines show that heat is mainly extracted from the lower-left corner of the enclosure, and that heat reaches the cold wall along a large portion of its length. Heat leaving the remaining portion of the hot wall reaches the cold wall just on a short region near its upper-right corner. The flow structure is also observed on the heatlines, with a clockwise vortex near the hot left vertical wall.

Results for $\theta = 30°$, $Ra_T = 100$, $H/L = 0.5$ and combined global heat and mass flows are presented in Fig. 4a for $N = 2$ and in Fig. 4b for $N = 5$. Main changes from Fig. 2 to 3a are due to the increase on the buoyancy term and to the change on H/L. Flow is more intense, the temperature and concentration gradients are higher near the vertical walls, and heat and mass transfer increases as N increases. As N increases, heat flows in a narrow region close to the top inclined wall of the enclosure. Numerical values of the heatfunction and massfunction confirm that heat and mass transfer increase. In what concerns temperature and concentration fields, as $Le = 0.8 \approx 1$, there are no major differences on these fields, as well as on the heatfunction and massfunction fields.

Results for the situation with $H/L = 0.5$, $\theta = 30°$, $Ra_T = 100$, $N = 5$ and opposite global heat and mass flows are presented in Fig. 5. The main contribution for buoyancy is due to concentration, the highest concentration level occurring at the right vertical wall. Thus, the natural convection induced flow presents a structure composed by counter-clockwise vortexes. In fact, streamlines present a flow structure with a main counter-clockwise vortex with two minor interior counter-clockwise vortexes near the upper-left and lower-right corners of the enclosure. The main flow visiting the neighboring of the vertical walls takes place through thin regions adjacent to the upper and lower inclined walls of the enclosure. Marked stratification is observed on the temperature and concentration fields, their contour plots being markedly horizontal and *parallel* to each other in a large portion of the central part of the enclosure. The intense temperature gradients are present near the upper-left and lower-right corners, the main heat and mass transfer processes occurring in such regions. It is observed from the heatlines that heat flows from the left to the right vertical wall through a thin region adjacent to the lower inclined wall. This is a direct consequence of the natural convection resulting counter-clockwise rotating flow. Due to this flow structure and to the imposed concentration boundary conditions, mass transfer takes place from the right to the left vertical wall through a thin region adjacent to the upper inclined wall of the enclosure, as clearly shown by the masslines.

3.3. Heat and mass transfer parameters

Global Nusselt number for the situation of no solute transfer ($N = 0$) is presented in Fig. 6a–c, as function of the inclination angle θ and of the ratio H/L, for Darcy-modified Rayleigh numbers of 25, 50 and 100, respectively. When $Ra_T = 25$, similar behaviors are observed for $H/L = 0.1$ and for $H/L = 0.2$, the Nusselt number for $H/L = 0.2$ being always greater than for $H/L = 0.1$. For low values of θ ($\theta \approx -60°$) and high values of θ ($\theta \approx 60°$) the global Nusselt number is nearly the same, and it is also nearly the same for $H/L = 0.1$ and for $H/L = 0.2$. Over all the $-60°$ to $60°$ range for θ, the global Nusselt number is only slightly greater than 1. When H/L changes from 0.2 to 0.5, the Nusselt number increases for any value of θ. It is observed the existence of a maximum Nusselt number for θ near 30°. The $H/L = 1$ Nusselt number presents a different behavior with the inclination angle θ. It considerably increases for the considered extreme values of θ, and exhibits a minimum for θ near $-10°$.

Denominator $(H/L)\cos\theta$ in the definition of the Nusselt and Sherwood numbers [Eqs. (19) and (20)] results from the better description of reality as H/L decreases but, due to the presence of $\cos\theta$, global Nusselt and Sherwood numbers can increase two times for the considered extreme values of θ.

In Fig. 6b is presented the Nusselt number as function of θ and H/L for $Ra_T = 50$. Changing from $Ra_T = 25$ to $Ra_T = 50$ results into a general increase on the Nusselt number for any value of inclination angle θ. The main change on the behavior of Nusselt with θ is given by the existence of marked maximum values of Nusselt number for $H/L = 0.2$ and $H/L = 0.5$, the greatest value corresponding to $H/L = 0.5$ and θ near 40°. In this case, it is evident the thermal diode effect of the parallelogrammic enclosure filled with a fluid-saturated porous medium, the Nusselt number for some positive values of θ being some times higher than the Nusselt number for negative values $-\theta$. Looking for

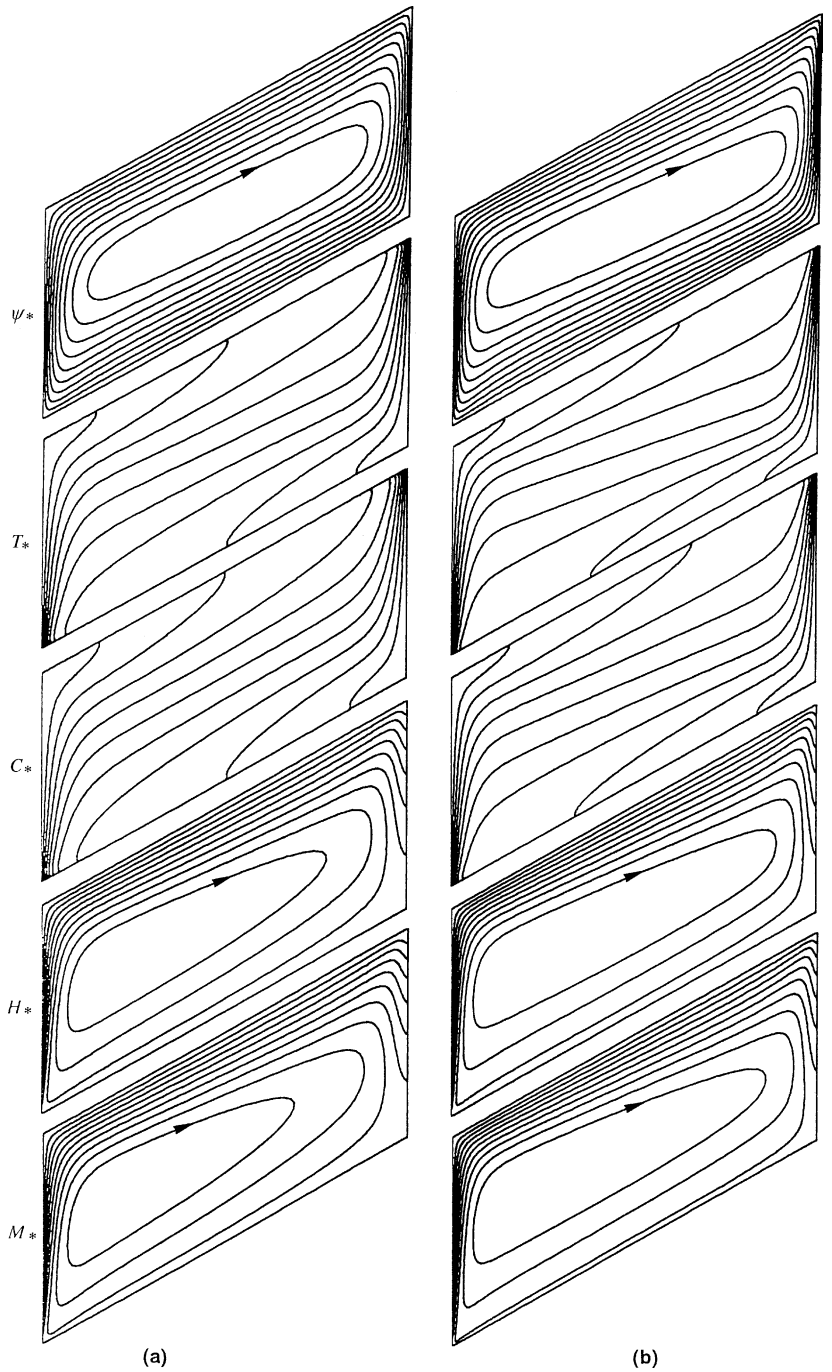

Fig. 4. Streamlines (top), isotherms (top-1) isoconcentration (top-2), heatlines (top-3) and masslines (bottom), for combined global heat and mass flows, $Le = 0.8$, $H/L = 0.5$, $Ra_T = 100$, and $\theta = 30°$ for (a) $N = 2$ ($\psi_{*,\min} = -13.18$, $\psi_{*,\max} = 0.00$, $\Delta\psi_* = 1.32$; $\Delta T_* = 0.10$, $\Delta C_* = 0.10$; $H_{*,\min} = -3.55$, $H_{*,\max} = 6.57$, $\Delta H_* = 1.01$; $M_{*,\min} = -3.62$, $M_{*,\max} = 6.82$, $\Delta M_* = 1.04$); and (b) $N = 5$ ($\psi_{*,\min} = -22.11$, $\psi_{*,\max} = 0.00$, $\Delta\psi_* = 2.21$; $\Delta T_* = 0.10$; $\Delta C_* = 0.10$; $H_{*,\min} = -5.69$, $H_{*,\max} = 10.81$, $\Delta H_* = 1.65$; $M_{*,\min} = -5.49$, $M_{*,\max} = 11.53$, $\Delta M_* = 1.70$).

practical applications, positive values of θ allow heat transfer promoters, and negative values of θ allow thermal insulation effect (for the specified temperature boundary conditions). The Nusselt number for $H/L = 1$

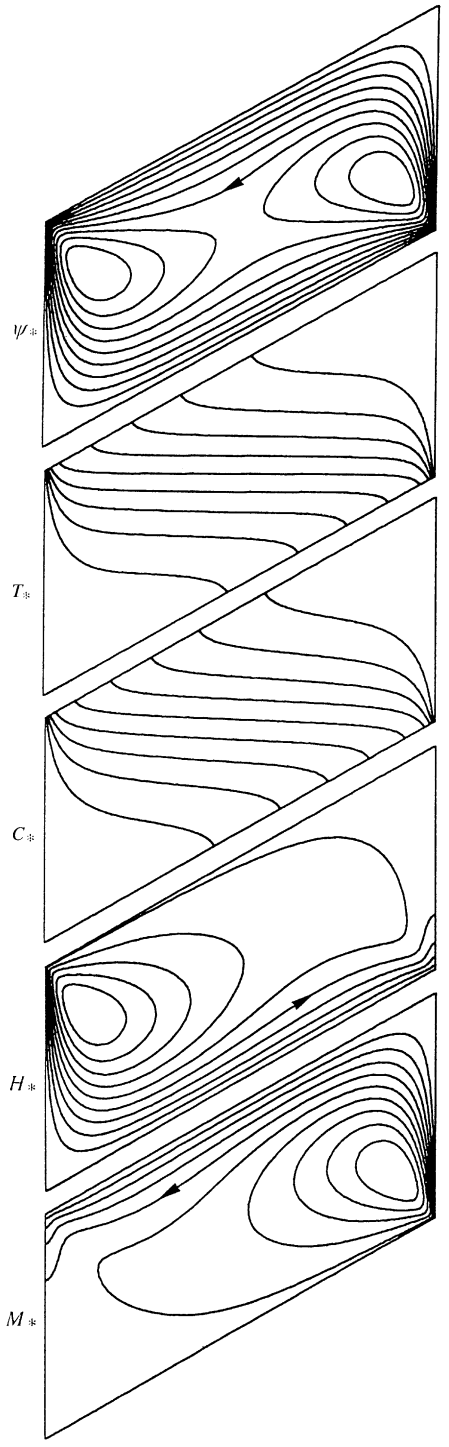

Fig. 5. Streamlines (top), isotherms (top-1) isoconcentration (top-2), heatlines (top-3) and masslines (bottom), for opposite global heat and mass flows, $Le = 0.8$, $H/L = 0.5$, $Ra_T = 100$, and $\theta = 30°$ for $N = 5$ ($\psi_{*,\min} = 0.00$, $\psi_{*,\max} = 4.64$, $\Delta\psi_* = 0.46$; $\Delta T_* = 0.10$; $\Delta C_* = 0.10$; $H_{*,\min} = 0.00$, $H_{*,\max} = 4.36$, $\Delta H_* = 0.44$, $M_{*,\min} = -2.06$, $M_{*,\max} = 2.39$, $\Delta M_* = 0.45$).

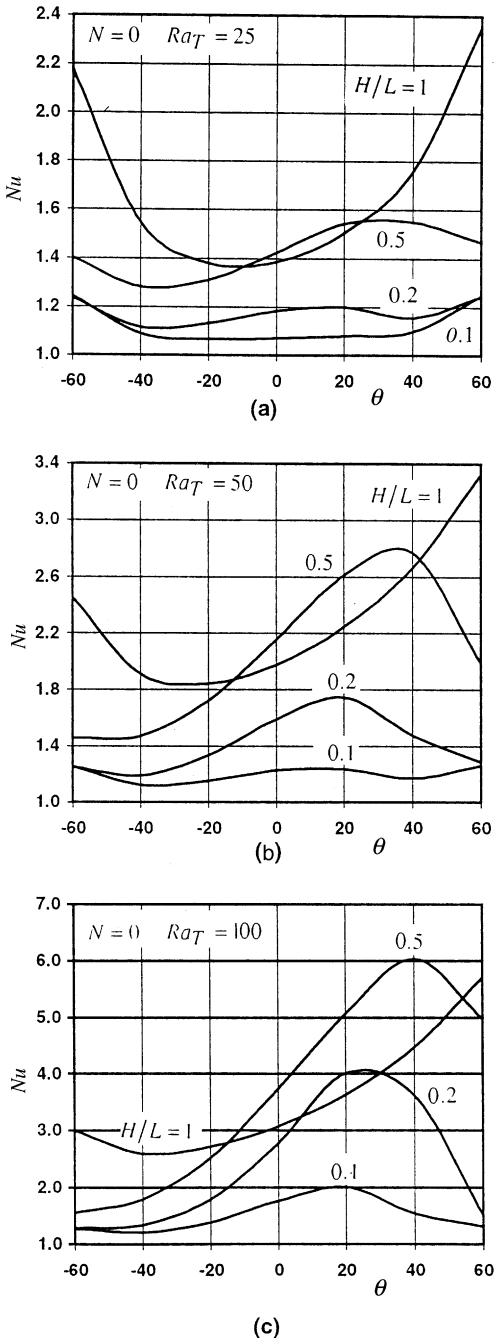

Fig. 6. Global Nusselt number versus inclination angle θ and ratio H/L for the situation of non-solute transfer ($N = 0$) and (a) $Ra_T = 25$; (b) $Ra_T = 50$; and (c) $Ra_T = 100$.

is higher for $Ra_T = 50$ than for $Ra_T = 25$, the maximum Nusselt number occurring for θ near $-30°$.

Results for $Ra_T = 100$ and $N = 0$ are presented in Fig. 6c. When compared with results for $Ra_T = 50$, it is observed a small increase on the Nusselt number for low

values of θ and a noticeable increase of the Nusselt number for positive and high values of θ. For $H/L = 0.1$, $H/L = 0.2$ and $H/L = 0.5$ it is evident the existence of maximum Nusselt numbers, greater values of the Nusselt number corresponding to greater values of H/L and θ, for θ in the range 20–40°. For $H/L = 1$ it is observed a general increase on the global Nusselt number when compared with the situation for $Ra_T = 50$, which exhibits a minimum value for θ near −40°. The thermal diode effect is evident, this effect increasing as increases the ratio H/L, for $H/L \leqslant 0.5$. For $H/L = 0.5$, the ratio $[(Nu)_\theta/(Nu)_{-\theta}]_{max}$ can reach values as high as nearly 4. For small values of H/L and for $\theta < -30°$, the Nusselt number is almost constant and independent of θ. The obtained results for $\theta = 0$ can be compared with those presented by Bejan [19] for this same situation, and a good agreement is observed.

The main advantage of using parallelogrammic enclosures to obtain insulation systems can be analyzed at this point. If one considers a vertical panel obtained by assembling n parallelogrammic enclosures, the heat transferred through the panel is obtained as

$$\dot{Q}(\theta, H/L) = nNu(\theta, H/L)k\frac{(T_H - T_L)}{L}H\cos\theta \tag{21}$$

Considering two panels 1 and 2, with the same width and composed by n enclosures with the same height H, it is imposed that $L_1\cos\theta_1 = L_2\cos\theta_2$ and the ratio between the heat transferred by such panels can be expressed as

$$\frac{\dot{Q}(\theta_1, H/L_1)}{\dot{Q}(\theta_2, H/L_2)} = \frac{Nu(\theta_1, H/L_1)}{Nu[\theta_2, (H/L_1)(\cos\theta_2/\cos\theta_1)]}\left(\frac{\cos\theta_1}{\cos\theta_2}\right)^2 \tag{22}$$

For the situation with $Ra_T = 100$, a square enclosure with $\theta_1 = 0°$ and $H/L_1 = 1$, and the parallelogramic enclosure with $\theta_2 = -60°$ and $H/L_2 = (H/L_1)(\cos\theta_2/\cos\theta_1) = 0.5$, one obtains from Fig. 6c that $\dot{Q}(0°, 1)/\dot{Q}(-60°, 0.5) \approx 8.27$, that is, the use of such a parallelogrammic enclosure significantly reduces the global heat transfer through the panel when compared with the panel obtained by assembling square enclosures with the same width.

Similar results can also be obtained for the parallelogrammic enclosures acting as heat transfer promoters, when compared with the rectangular enclosure, for positive values of the inclination angle θ. This result is obvious for square and parallelogrammic enclosures with equal length L.

The obtained behavior of the parallelogrammic enclosure for heat transfer also applies for mass transfer. The diode effect is thus a characteristic of the parallelogrammic shape, which can be used with great advantage for the inhibition or for the promotion of the heat and/or mass transfer processes through such enclosures, taken individually or assembled in the form of panels.

A physical explanation can be given for the thermal diode effect. For positive values of θ the hot fluid moves upwards and reaches the inclined upper wall, which has a favorable inclination, allowing some tangentiality to the flow flowing along the inclined wall towards the cold wall. The same applies also for the descending cold fluid on the neighboring of the opposite vertical wall. The flow is intense and the thermal gradients near the vertical walls are high, thus resulting into high global heat transfer rates. For negative values of θ, the inclined wall has a non-favorable inclination, and the fluid tends to be trapped on the top of the hot wall and on the bottom of the cold wall of the enclosure, with a resulting marked thermal stratification there. The flow is less intense and the thermal gradients are smaller near the vertical walls, thus resulting into lower heat transfer rates. This same physical explanation applies also for the mass transfer diode effect, when solute transfer is present.

Results for combined global heat and mass flows and $N = 2$ are presented in Fig. 7a–c for the same values of Ra_T of 25, 50 and 100, respectively. As the solute mass transfer is present, analysis includes also the global Sherwood number. In general terms, it can be observed that as $Le = 0.8 \approx 1$, there are no significant differences between the behavior and the numeric values of the global Nusselt and Sherwood numbers. For $Ra_T = 25$ it is observed an increase on the Nusselt number for intermediate values of θ relative to the non-solute transfer situation as illustrated in Fig. 6a. It is also observed the existence of marked maximum values of the Nusselt and Sherwood numbers for $H/L = 0.1$, $H/L = 0.2$ and $H/L = 0.5$, which occur nearly in the range $10° < \theta < 40°$. For $H/L = 1$, the Nusselt and Sherwood numbers maintain their increases for low and high values of θ, the numeric values for θ being higher than these corresponding to $-\theta$, and the minimum Nusselt and Sherwood numbers correspond to $\theta \approx -30°$. For $Ra_T = 50$, in Fig. 7b, remains essentially the analysis made to Fig. 6b, now enlarged to include the Sherwood number. When $Ra_T = 100$, in Fig. 7c, there are marked maxima on the Nusselt and Sherwood numbers for $H/L = 0.1$ and for $H/L = 0.2$, the transfer parameters for $H/L = 0.2$ being higher than those for $H/L = 0.1$. For $H/L = 0.5$ and $H/L = 1$ it is observed a monotonic increase on the Nusselt and Sherwood numbers when θ increases. However, for $\theta \gtrsim -20°$, the transfer parameters corresponding to $H/L = 0.5$ are higher than those corresponding to $H/L = 1$, this relation being inverted for $\theta \lesssim -20°$.

The situation corresponding to combined heat and mass flows and $N = 5$ is presented in Fig. 8a–c for $Ra_T = 25$, $Ra_T = 50$ and $Ra_T = 100$, respectively. Fig. 8c represents the situation with the highest source term considered in the vertical momentum equation, with

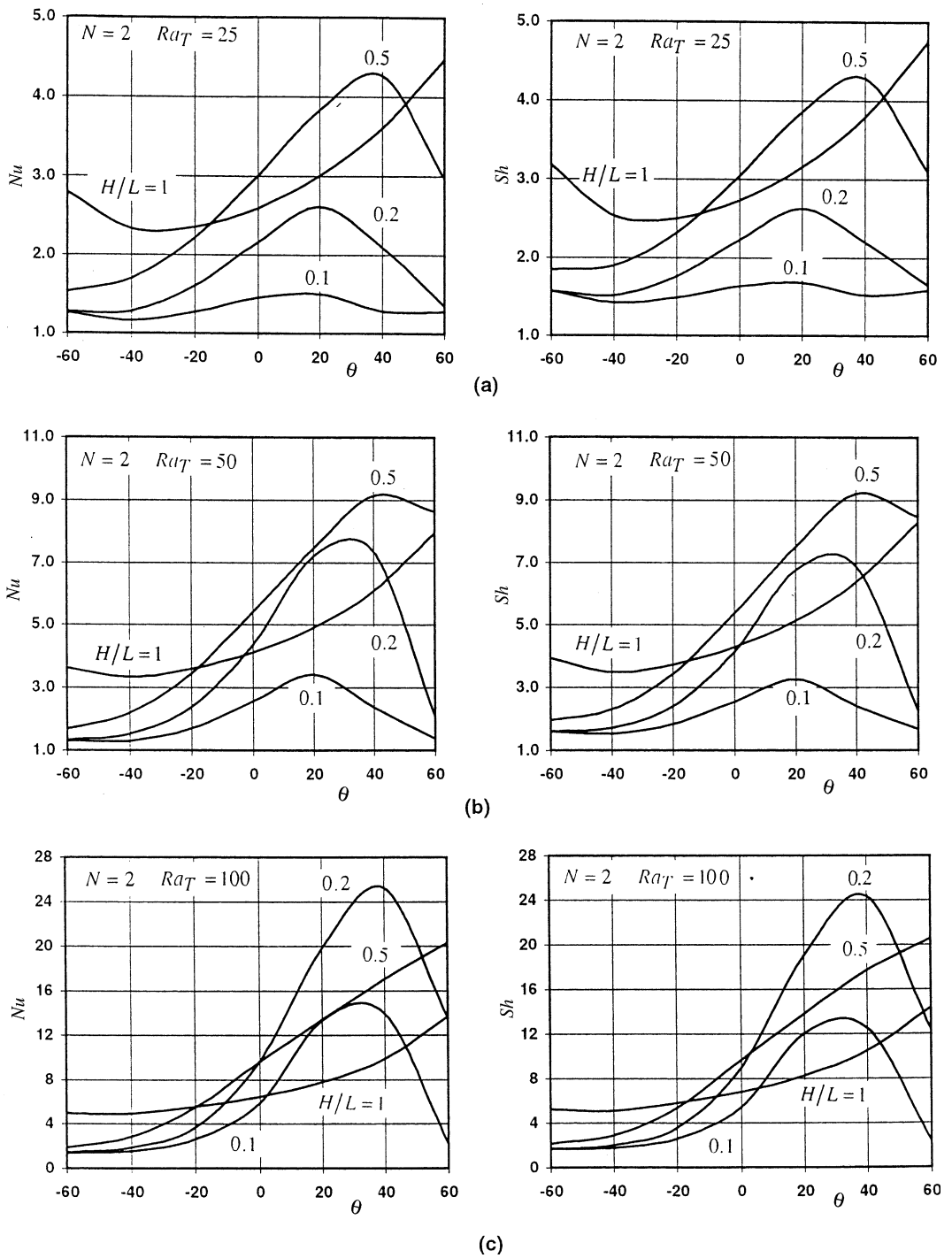

Fig. 7. Global Nusselt (left) and Sherwood (right) numbers versus inclination angle θ and ratio H/L for the situation of combined global heat and mass transfer with $N = 2$ and (a) $Ra_T = 25$; (b) $Ra_T = 50$; and (c) $Ra_T = 100$.

high numerical values for the Nusselt and Sherwood numbers, for high values of θ. In this case, the maximum heat transfer parameters are obtained for $H/L = 0.1$, for θ near 40°. For $H/L = 0.2$, $H/L = 0.5$, and $H/L = 1$ there are not observed maxima, and the transfer parameters have an essentially monotonically increasing

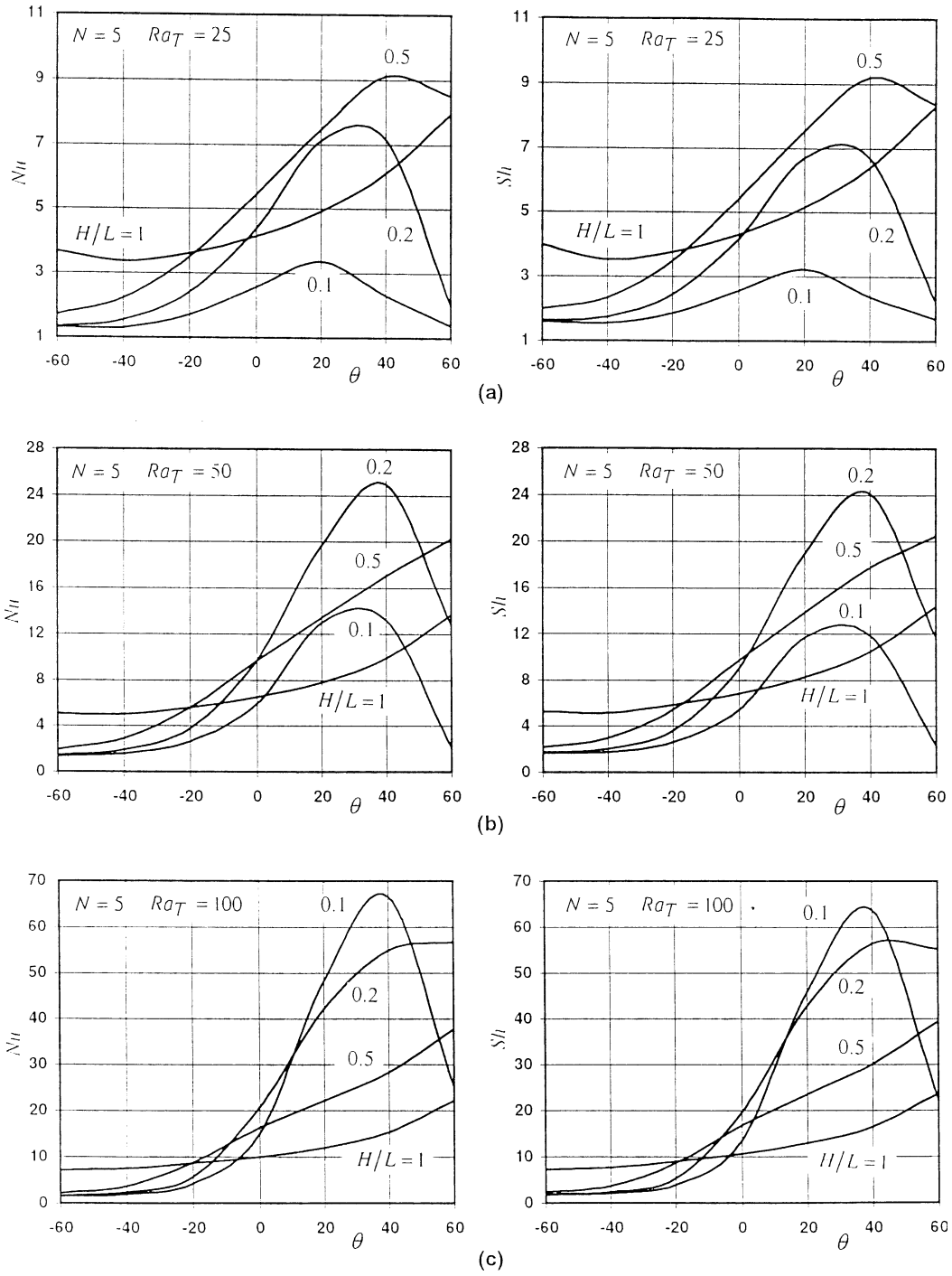

Fig. 8. Base legend as for Fig. 7, but for $N = 5$.

behavior with θ. In this case, the thermal diode effect for $H/L = 0.1$, evaluated as $[(Nu)_{\theta}/(Nu)_{-\theta}]_{\max}$ can reach values as high as nearly 50, which is remarkable and demonstrates the high potential of the parallelogrammic enclosures. The same applies similarly to the mass transfer diode effect of the parallelogrammic enclosure. It should be mentioned that the heat and mass transfer diode effects increase as increases the vertical momentum source term, the transfer parameters for low values of θ remaining essentially unchanged.

Results for opposite global heat and mass flows and $N = 5$ are presented in Fig. 9a–c, for $Ra_T = 25$, $Ra_T = 50$ and $Ra_T = 100$, respectively. The vertical momentum source term is conditioned essentially by the concen-

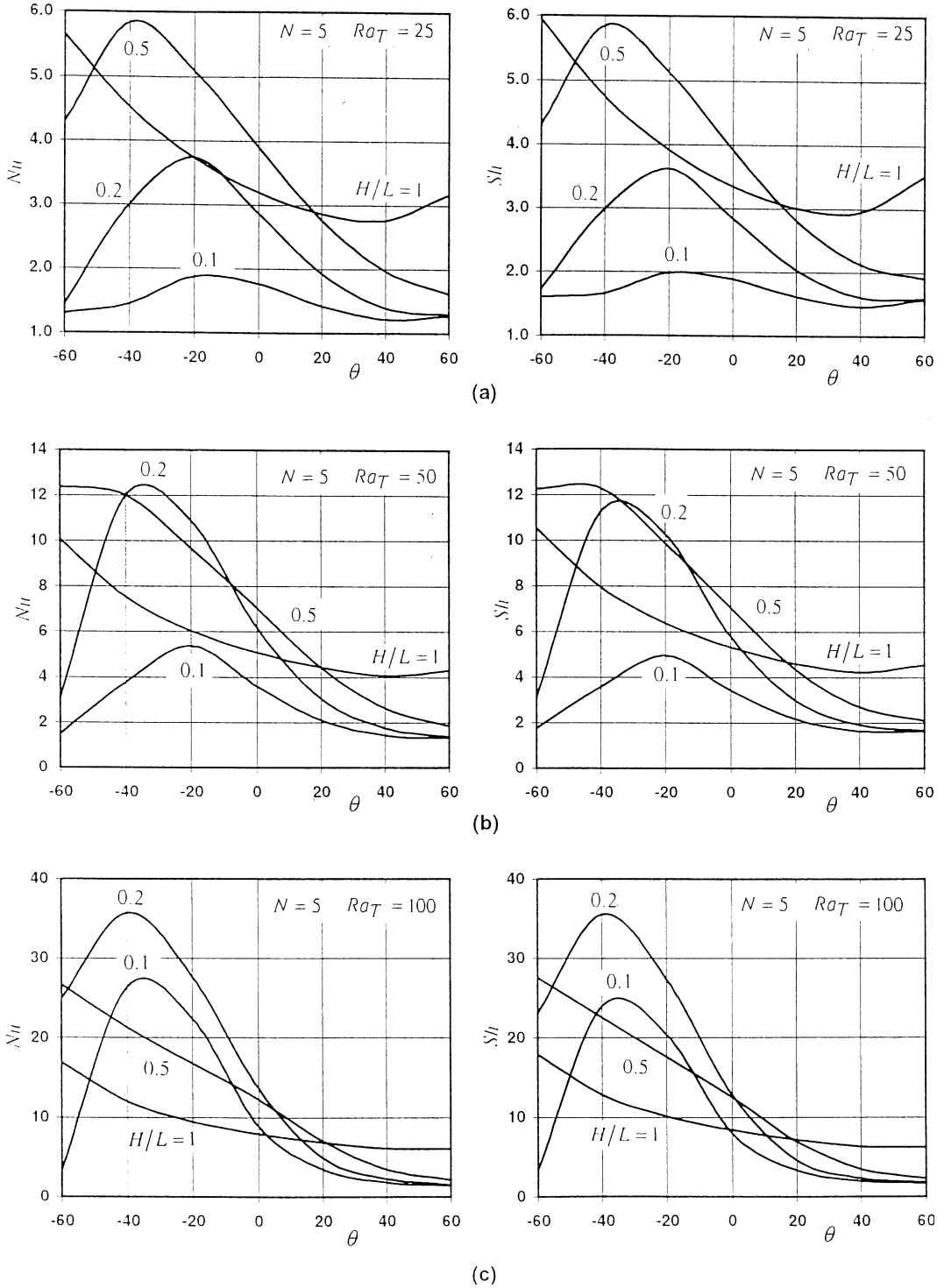

Fig. 9. Global Nusselt (left) and Sherwood (right) numbers versus inclination angle θ and ratio H/L for the situation of opposite global heat and mass transfer with $N = 5$ and (a) $Ra_T = 25$; (b) $Ra_T = 50$; and (c) $Ra_T = 100$.

tration field, which has its maximum at the right vertical wall of the enclosure. From the physical explanation given for the heat and mass transfer diode effects, the favorable inclination corresponds now to negative values of θ, and the non-favorable situation corresponds to positive values of θ. For $Ra_T = 25$, in Fig. 9a, there are marked maximum values of the Nusselt and Sherwood numbers for $H/L = 0.1$, $H/L = 0.2$ and $H/L = 0.5$, all for negative values of θ, the highest heat and mass transfer parameters occurring for $H/L = 0.5$. When Ra_T changes from 25 to 50, this in Fig. 9b, there is a considerable increase on the heat and mass transfer parameters for negative values of θ, with marked maxima for $H/L = 0.1$ and $H/L = 0.2$. The region of the figure corresponding to high values of θ remains essentially unchanged. For $Ra_T = 100$, in Fig. 9c, higher heat and mass transfer parameters are obtained for lower values of θ, and lower heat and mass transfer parameters are obtained for higher values of θ. In this case, there are also noticeable heat and mass transfer diode effects. Their physical explanation remains the same as for the situation of combined global heat and mass flows, the highest transfer parameters occurring now for low values of θ and the minimum values of the heat and mass transfer parameters occur for high values of θ.

From the dependence of the Nusselt and Sherwood numbers on θ and H/L, and from the exhibited maxima of these transfer parameters, additional work remains to be made in what concerns the finding of relationships to give $(Nu, Sh)_{max}$ as function of θ and H/L for a given Darcy-modified Rayleigh number.

4. Conclusions

Many heat and/or mass transfer elements can be made of enclosures filled with fluid-saturated porous media. Parallelogrammic shape is very attractive as the basic shape for the enclosures to build, by assembly, more complete and complex structures that should present high and versatile heat and/or mass transfer performances. As many construction elements, in the form of enclosures, are subject to heat and mass transfer and are, in many situations, filled with moist air-saturated porous media, present study deals mainly with such systems. Even if the presented results refer to moist air only, the presented model is quite general, and the non-solute transfer or the isothermal situations are simple particular cases.

In terms of flow structure, temperature levels and concentration levels, strong changes occur in the parallelogrammic enclosure when changes are made on the Darcy-modified Rayleigh number, on the inclination angle and/or on the aspect ratio of the enclosure. Increasing the source term of the vertical momentum equation, by increasing the Darcy-modified Rayleigh number or by increasing the buoyancy ratio, always leads to increases on the heat and/or mass transfer performances of the enclosure. Such increases are, however, strongly dependent on the aspect ratio of the enclosure and on the inclination angle. Very different behaviors are obtained for the combined or opposite global heat and mass flows that cross the parallelogrammic enclosure. This is of special interest because, in many practical situations, both situations can equally occur.

When dealing with construction elements filled with moist air-saturated porous media, special attention needs to be given to the temperature and concentration levels at each point of the enclosure, as they can lead to condensation conditions inside the enclosure. Additionally, the porous matrix can act as a set of condensation nuclei, the condensation phenomenon occurring more easily than in an enclosure filled with a single fluid. With careful control of the temperature and concentration levels, such (usually damaging) condensation conditions can be avoided.

In what concerns the heat and/or mass transfer performances of the parallelogrammic enclosure, some main aspects should be mentioned. Selected combinations of the aspect ratio and inclination angle can lead to considerably high heat and/or mass flows through the enclosure, and some combinations of these parameters can even lead to the maximum allowable heat and/or mass transfer. It is thus present a maximum transfer performance, which is of crucial importance when the parallelogrammic enclosure is to be used as a transfer promoter. However, other selected inclination angles, of opposite sign from the foregoing ones, can lead to essentially unchanged poor transfer performances of the enclosure. Notable is the transfer diode effect of the parallelogrammic enclosure: for a given aspect ratio, the ratio between the maximum of the transfer parameters to the respective minimum transfer parameters can be of some tenths. It is this marked directional transfer behavior of the parallelogrammic enclosure that, adequately conjugated with the temperature and concentration boundary conditions, gives to this shape so much interest and so high potential to be used in systems where heat and/or mass transfer processes are present.

Many of the conclusions made on the heat and/or mass transfer characteristics and performances of the parallelogrammic enclosures filled with fluid-saturated porous media are also valid for the similar parallelogrammic enclosures without any porous media, and filled with a single fluid only.

References

[1] P. Nithiarasu, K.N. Seetharamu, T. Sundararajan, Double-diffusive natural convection in an enclosure filled with

fluid-saturated porous medium: a generalized non-Darcy approach, Numer. Heat Transfer, Part A 30 (1996) 413–426.
[2] M. Karimi-Fard, M.C. Charrier-Mojtabi, K. Vafai, Non-Darcian effects on double-diffusive convection within a porous medium, Numer. Heat Transfer, Part A 31 (1997) 837–852.
[3] A.J. Chamkha, Double-diffusive convection in a porous enclosure with cooperating temperature and concentration gradients and heat generation or absorption effects, Numer. Heat Transfer, Part A 41 (2002) 65–87.
[4] F. Alavyoon, On natural convection in vertical porous enclosures due to prescribed fluxes of heat and mass at the vertical boundaries, Int. J. Heat Mass Transfer 36 (10) (1993) 2479–2498.
[5] K. Khanafer, K. Vafai, Double-diffusive mixed convection in a lid-driven enclosure filled with a fluid-saturated porous medium, Numer. Heat Transfer, Part A 42 (2002) 465–486.
[6] K. Benhadji, P. Vasseur, Double diffusive convection in a shallow porous cavity filled with a non-Newtonian fluid, Int. Commun. Heat Mass Transfer 28 (6) (2001) 763–772.
[7] Y. Masuda, M. Yoneya, T. Ikeshoji, S. Kimura, F. Alavyoon, T. Tsukada, M. Hozawa, Oscillatory double-diffusive convection in a porous enclosure due to opposing heat and mass fluxes on the vertical walls, Int. J. Heat Mass Transfer 45 (6) (2002) 1365–1369.
[8] M. Mamou, P. Vasseur, E. Bilgen, Multiple solutions for double-diffusive convection in a vertical porous enclosure, Int. J. Heat Mass Transfer 38 (10) (1995) 1787–1798.
[9] L. Kalla, M. Mamou, P. Vasseur, L. Robillard, Multiple solutions for double-diffusive convection in a shallow porous cavity with vertical fluxes of heat and mass, Int. J. Heat Mass Transfer 44 (23) (2001) 4493–4504.
[10] P. Bear, A. Khalili, Double-diffusive natural convection in an anisotropic porous cavity with opposing buoyancy forces: multi-solutions and oscillations, Int. J. Heat Mass Transfer 45 (15) (2002) 3205–3222.
[11] K.C. Chung, L.M. Trefethen, Natural convection in a vertical stack of inclined parallelogrammic cavities, Int. J. Heat Mass Transfer 25 (2) (1982) 277–284.
[12] N. Seki, S. Fokosako, A. Yamaqushi, An experimental study of free convective heat transfer in a parallelogrammic enclosure, ASME J. Heat Transfer 105 (1983) 433–439.
[13] J.M. Hyun, B.S. Choi, Transient natural convection in a parallelogram-shaped enclosure, Int. J. Heat Fluid Flow 11 (2) (1990) 129–134.
[14] V.A.F. Costa, A.R. Figueiredo, L.A. Oliveira, Convecção natural em cavidades paralelogrâmicas, in: Proceedings of the I Congreso Iberoamericano de Ingeniería. Mecánica, E.T.S. Ingenieros Industrials, Madrid, vol. 2, 1993, pp. 255–260.
[15] M.-R. Zugari, J.-J. Vullierme, Étude numérique du transfert de chaleur dans une cavité de forme parallélogrammatique et inclinée, à parois passives minces, Compt. Rend. Acad. Sci. Paris 319 (Série II) (1994) 1157–1163.
[16] K.D. Aldridge, H. Yao, Flow features of natural convection in a parallelogrammic enclosure, Int. Commun. Heat Mass Transfer 28 (7) (2001) 923–931.
[17] V.A.F. Costa, Double-diffusive natural convection in parallelogrammic enclosures, Int. J. Heat Mass Transfer, submitted.
[18] V.A.F. Costa, Unification of the streamline, heatline and massline methods for the visualization of two-dimensional transport phenomena, Int. J. Heat Mass Transfer 42 (1) (1999) 27–33.
[19] A. Bejan, Convection Heat Transfer, second ed., Wiley, New York, 1995.
[20] E.R.G. Eckert, R.M. Drake Jr., Analysis of Heat and Mass Transfer, McGraw-Hill, New York, 1972.
[21] A. Bejan, Heat Transfer, Wiley, New York, 1993.
[22] D.A. Nield, A. Bejan, Convection in Porous Media, second ed., Springer Verlag, New York, 1999.
[23] M. Kaviany, Principles of Heat Transfer in Porous Media, Springer Verlag, New York, 1991.
[24] V.A.F. Costa, L.A. Oliveira, A.R. Figueiredo, A control volume based finite element method for three-dimensional incompressible turbulent fluid flow, heat transfer, and related phenomena, Int. J. Numer. Methods Fluids 21 (7) (1995) 591–613.
[25] V.A.F. Costa, A.C.M. Sousa, Modeling of flow and thermo-kinetics during the cure of thick laminated composites, Int. J. Thermal Sci. 42 (1) (2003) 15–22.
[26] V.A.F. Costa, M.S.A. Oliveira, A.C.M. Sousa, Control of laminar natural convection in differentially heated square enclosures using solid inserts at the corners, Int. J. Heat Mass Transfer 46 (18) (2003) 3521–3528.
[27] V.A.F. Costa, Unified streamline, heatline and massline methods for the visualization of two-dimensional heat and mass transfer in anisotropic media, Int. J. Heat Mass Transfer 46 (8) (2003) 1309–1320.
[28] V.A.F. Costa, Double diffusive natural convection in a square enclosure with heat and mass diffusive walls, Int. J. Heat Mass Transfer 40 (17) (1997) 4061–4071.